BRNO UNIVERSITY OF TECHNOLOGY

VYSOKÉ UČENÍ TECHNICKÉ V BRNĚ

FACULTY OF MECHANICAL ENGINEERING

FAKULTA STROJNÍHO INŽENÝRSTVÍ

INSTITUTE OF PHYSICAL ENGINEERING

ÚSTAV FYZIKÁLNÍHO INŽENÝRSTVÍ

DOUBLE-GATE BIOSENSOR OF GLUCOSE BASED ON FUNCTIONALIZED GRAPHENE

DVOUHRADLOVÝ BIOSENZOR GLUKÓZY NA BÁZI FUNKCIONALIZOVANÉHO GRAFENU

BACHELOR'S THESIS

BAKALÁŘSKÁ PRÁCE

AUTHOR

AUTOR PRÁCE

Michaela Malatinová

SUPERVISOR

VEDOUCÍ PRÁCE

doc. Ing. Miroslav Bartošík, Ph.D.

BRNO 2022

BRNO UNIVERSITY OF TECHNOLOGY
FACULTY OF MECHANICAL ENGINEERING

Assignment Bachelor's Thesis

Institut:	Institute of Physical Engineering
Student:	**Michaela Malatinová**
Degree programm:	Physical Engineering and Nanotechnology
Branch:	no specialisation
Supervisor:	**doc. Ing. Miroslav Bartošík, Ph.D.**
Academic year:	2021/22

As provided for by the Act No. 111/98 Coll. on higher education institutions and the BUT Study and Examination Regulations, the director of the Institute hereby assigns the following topic of Bachelor's Thesis:

Double–gate biosensor of glucose based on functionalized graphene

Brief Description:

Thanks to its unique properties, especially: high mobility of charge carriers, compatibility with biological substances and changes in electrical properties caused by the influence of individual adsorbed biochemical molecules, graphene is an almost ideal material for use in biosensors [1]. Its main disadvantage in this area is the fact that graphene reacts to any adsorbed molecule indiscriminately through changes in resistance and thus does not show in itself a sufficient selectivity in the detection of a specific biochemical compound. The aim of this work is to overcome this disadvantage through the appropriate functionalization of graphene so that the sensor based on functionalized graphene reacts selectively only to the selected biochemical substance [2–6] and research the possibilities of common upper electrolytic and bottom solid–state gate electrode.

Bachelor's Thesis goals:

1. Literature retrieval of the mentioned issue with emphasis on suitable initial functionalization of graphene and detected biochemical compound.
2. Graphene functionalization and verification of functionalization efficiency (Raman spectroscopy, XPS, transport measurements).
3. Design and manufacture of a suitable graphene sensor based on functionalized graphene.
4. Measurement of the transport response of a graphene sensor to a suitable biochemical substance.
5. Analysis of results with regard to the effectiveness of functionalization, sensor sensitivity and especially its selectivity.
6. Study the influence of both mentioned gate electrodes.

Recommended bibliography:

SCHEDIN, F., A. K. GEIM, S. V. MOROZOV, E. W. HILL, P. BLAKE, M. I. KATSNELSON a K. S. NOVOSELOV. Detection of individual gas molecules adsorbed on graphene. Nature Materials. 2007, 6(9), 652-655. DOI: 10.1038/nmat1967.

SHAO, Y., J. WANG, H. WU, J. LIU, I. A. AKSAY, Y. LIN. Graphene Based Electrochemical Sensors and Biosensors: A Review. Electroanalysis. 2010, 22(10), 1027-1036. DOI: 10.1002/elan.200900571.

NAG, A., A. MITRA, S. C. MUKHOPADHYAY. Graphene and its sensor-based applications: A review. Sensors and Actuators A: Physical. 2018, 270, 177-194. DOI: 10.1016/j.sna.2017.12.028.

KWAK, Y. H., D. S. CHOI, Y. N. KIM, H. KIM, D. H. YOON, S. S. AHN, J. W. YANG, W. S. YANG, S. SEO. Flexible glucose sensor using CVD-grown graphene-based field effect transistor. Biosensors and Bioelectronics. 2012, 37(1), 82-87. DOI: 10.1016/j.bios.2012.04.042.

SHAN, C., H. YANG, J. SONG, D. HAN, A. IVASKA, L. NIU. Direct Electrochemistry of Glucose Oxidase and Biosensing for Glucose Based on Graphene. Analytical Chemistry. 2009, 81(6), 2378-2382. DOI: 10.1021/ac802193c.

ZHU, Zanzan. An Overview of Carbon Nanotubes and Graphene for Biosensing Applications. Nano-Micro Letters. 2017, 9(3), 1-24. DOI: 10.1007/s40820-017-0128-6.

Deadline for submission Bachelor's Thesis is given by the Schedule of the Academic year 2021/22

In Brno,

L. S.

prof. RNDr. Tomáš Šikola, CSc. Director of the Institute	doc. Ing. Jaroslav Katolický, Ph.D. FME dean

ABSTRACT

This bachelor's thesis studies functionalization of graphene with linker molecule pyrenebutanoic acid succinimidyl ester and the enzyme glucose oxidase for glucose detection by a biosensor. The functionalized graphene implemented as the channel in field-effect transistor was used for the fabrication of the biosensing device. The functionalization process was confirmed by Raman spectroscopy and Atomic Force Microscopy. The characterization of the sensor and its qualities were monitored using transfer curves and time response. The shift in Dirac point and its position were inspected in relation to different concentrations of glucose and efficiency of the functionalization. The choice of the gate electrode of the graphene field-effect transistor was investigated with respect to its possible impact on the measurement results.

ABSTRAKT

V tejto bakalárskej práci bola skúmaná funkcionalizácia grafénu s sukcinimidyl ester pyrenbutanovou kyselinou a enzýmom glukóza oxidáza pre detekciu glukózy biosenzorom. Funkcionalizovaný grafén bol implementovaný ako kanál v poľom riadenom tranzistore pre výrobu biodetekčného zariadenia. Proces funkcionalizácie potvrdila Ramanova spektroskopia a mikroskopia atomárných síl. Charakterizácia senzoru a jeho kvalít bola sledovaná pomocou transferových kriviek a časovej odozvy senzoru. Posun Diracovho bodu a jeho poloha boli analyzované v závislosti na rôznych koncentráciach glukózy s ohľadom na efektivitu funkcionalizácie. Výber hradlovej elektródy v grafénovom poľom riadenom tranzistore bol skúmaný vzhľadom na jeho možný dopad na výsledky merania.

KEYWORDS

functionalized graphene, sensor, field-effect transistor, Dirac point, glucose, glucose oxidase

KĽÚČOVÉ SLOVÁ

funkcionalizovaný grafén, senzor, poľom riadený tranzistor, Diracov bod, glukóza, glukóza oxidáza

MALATINOVÁ, M. *Double-gate biosensor of glucose based on functionalized graphene.* Brno: Vysoké učení technické v Brně, Fakulta strojního inženýrství, 2022. 43 s. Vedoucí práce doc. Ing. Miroslav Bartošík, Ph.D..

Author's Declaration

Author:	Michaela Malatinová
Author's ID:	216826
Paper type:	Bachelor's Thesis
Academic year:	2021/22
Topic:	Double-gate biosensor of glucose based on functionalized graphene

I declare that I have written this paper independently, under the guidance of the advisor and using exclusively the technical references and other sources of information cited in the paper and listed in the comprehensive bibliography at the end of the paper.

As the author, I furthermore declare that, with respect to the creation of this paper, I have not infringed any copyright or violated anyone's personal and/or ownership rights. In this context, I am fully aware of the consequences of breaking Regulation § 11 of the Copyright Act No. 121/2000 Coll. of the Czech Republic, as amended, and of any breach of rights related to intellectual property or introduced within amendments to relevant Acts such as the Intellectual Property Act or the Criminal Code, Act No. 40/2009 Coll. of the Czech Republic, Section 2, Head VI, Part 4.

Brno ....

author's signature*

*The author signs only in the printed version.

ACKNOWLEDGEMENT

I would like to thank my supervisor, doc. Ing. Miroslav Bartošík, Ph.D. for professional guidance, patience and mentorship during this process. I would also like to express gratitude to Ing. Martin Konečný. Ph.D., Bc. Daniel Lipták, Ing. Jakub Piastek, Bc. Linda Supalová and Ing. Vojtěch Švarc for their time, advice and insight provided along the way. Last but not least, I would like to thank my family, friends and classmates, for their ever-present support and love.

Contents

Introduction

Two dimensional graphene shows great promise as a biosensor material for targeting glucose due to its exceptional electrical conductivity, large specific surface area and possibility of functionalization. Sensors with selectivity and sensitivity to glucose are a key for detection of glucose in blood and can be use for diagnose and prevention of diabetes. Thus tremendous interests is to develop chemical sensor for glucose detection *in vivo*. Enzymeless sensors usually do not have sensitivity and also good enough selectivity. Therefore, glucose oxidase based glucose sensors became widely researched. Glucose oxidase has been known as an enzyme selective to glucose. Modified graphene in combination with structure defects can immobilize glucose oxidase. Graphene is utilized to promote electron transfer between the electrode and glucose oxidase. Both covalent and noncovalent methods can be used to functionalize graphene. The noncovalent method is preferred because it allows for preservation of graphene electronic properties.

Field-effect transistors (FETs), apart from their standard utilization in logical-switches and amplifiers, can be used as a special class of sensors, where the biological analytes is detected as a alteration in the electrical resistance of the sensor tuned by gate electrode. Recently the graphene field-effect transistors (GFETs) have been studied for biosensing applications because of graphene's biocompatibility .

In this work, the chemical vapor deposition (CVD) graphene was employed as a conductive channel in GFET noncovalently functionalized with 1-pyrenebutanoic acid succinimidyl ester and glucose oxidase to detect glucose. Theoretical part of the thesis deals with the proper functionalization methods, proper measurements techniques and state of the art of graphene based glucose sensors. The experimental part was focused on the verification of the functionalization process and the change in electrical measurements as a response to glucose detection.

1 Theoretical part

1.1 Graphene

Graphene is a two-dimensional material consisting of a single layer of carbon atoms, tightly packed to form a repeating pattern of hexagons. Previously the graphene was used to describe different carbon-based materials. However, in the last two decades graphene, formerly known as a theoretical model, became an object of wide interest when it was experimentally discovered in 2004 by Andre Geim and Konstantin Novoselov. Since, it was used in numerous applications. Especially in biomedical engineering, conversion and energy storage, sensors, and flexible electronics thanks to its large surface-to-volume ratio, specific optical properties, high carrier mobility, thermal conductivity and electric conductivity.

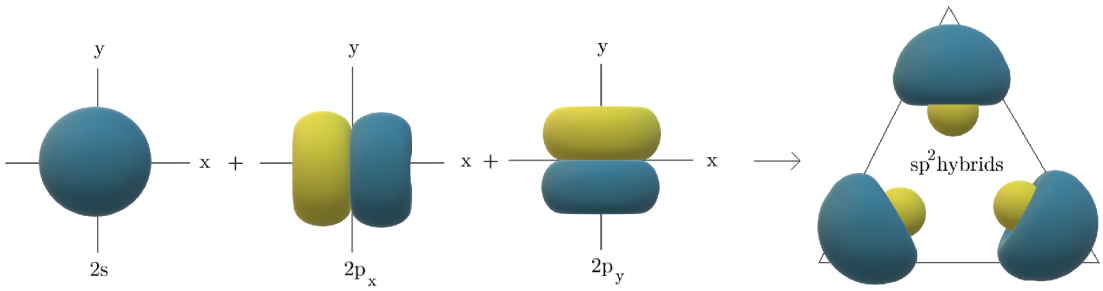

Fig. 1.1: The formation of sp^2 hybridization.

Carbon has a ground-state electronic configuration of $1s^2 2s^2 2p_x^1 2p_y^1 2p_z^0$. Carbon nucleus is surrounded by six electrons. Four of them are valence and form three types of hybridization, that is sp, sp^2 (see figure 1.1) and sp^3. When carbon atoms share sp^2 electrons with three of their neighboring atoms, they create a monolayer of graphene. Unit cell of graphene contains two carbon atoms as shown in figure 1.2 (b), the lattice constant is 2.46 Å for both unit-cell vectors $\mathbf{a_1}$ and $\mathbf{a_2}$. The stability of the planar ring can be attributed to the delocalization of the electrons. For two neighboring carbon atoms in sp^2 hybridization, π bond is created by $2p_z$ orbitals, perpendicular to the planar structure, and an in-plane σ bonds made up by 2s, $2p_x$ and $2p_y$ hybridized orbitals. The strong covalent σ bonds with length of 1,42 Å are responsible for the exceptional mechanical properties of graphene monolayer (such as Young's modulus of 1 TPa [2]). Every atom of graphene sheet is attached by

three σ-bonds to other atoms and adds one electron to a conduction band of the whole sheet.

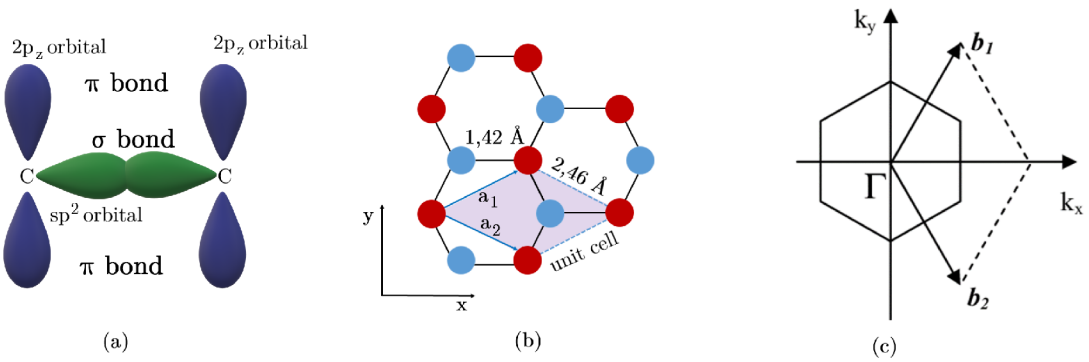

Fig. 1.2: Schematic representation of (a) the formation of σ and π bonds, (b) the lattice of graphene in real space and (c) the lattice in reciprocal space, reproduced from [3].

Graphene is a half-filled system, which means the valence band is completely filled. The electronic properties of the system are given by the spectrum close to the last filled states, determined by the Fermi level. In graphene it is given by the values of spectrum near the top of the valence band and the bottom of the conduction band. As seen in figure1.4, the valence and the conduction bands touch at specific points of reciprocal space that are called Dirac points (figure 1.4). As a result the graphene does not have an energy gap. Graphene can be considered as a zero-gap semiconductor with vanishing density of states in the Dirac points. The energy spectrum close to the Dirac points forms a conical shape, with positive (negative) values for conduction (valence) bands and is represented by equation:

$$E = \pm v_F p \tag{1.1}$$

where v_F is the Fermi velocity, p is the momentum, and E the energy. The Fermi velocity is $c/300$, c is the speed of light [4].

Although there is a whole class of 2D materials, the focus remains on graphene for its exceptional electronic qualities. The ambipolar field effect of graphene makes possible to change between holes and electrons. The mobility μ of charge carriers in graphene can reach up to $15000\,\mathrm{cm^2\,V^{-1}\,s^{-1}}$. Another indication of the system's high mobility is the quantum Hall effect which can be observed in graphene even at room temperature. Graphene's charge carrier dispersion relation mimics relativistic zero mass particles thus rather than using the Schrödinger equation for their description the Dirac equation is more suitable [5].

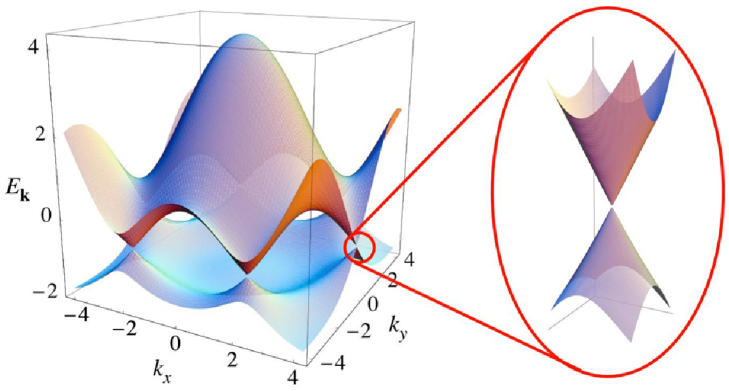

Fig. 1.3: Energy band spectrum in the hexagonal lattice of graphene (left) and detail of the energy bands with one Dirac point (right). Reproduced from [4].

1.1.1 Chemical vapor deposition

Graphene fabrication is a complex process. The main goal is to create low-cost graphene of good quality [6]. Graphene can be prepared using various methods, chemical vapour deposition became a widespread method for the production and preparation of graphene for numerous applications. The process of chemical vapour deposition consists of injecting volatile precursor gas into a vacuum chamber. Precursor gas is heated and breaks down to a coating. The coating bonds to the material surface and creates layer. The formation of graphene by CVD is built in a two-step process. Firstly, the incorporation or dilution of carbon into the metal substrate. Followed by carbon segregation into graphene induced by rapid cooling. In the most used graphene growing procedure, the camber containing copper foil is filled with methane and heated up to 1000 °C. When the methane molecules hit the copper foil, the carbon atoms attach to the surface. Allowing the film to grow directly on the surface, the film is mainly graphene with less than 5 % of the area being two or three layers of graphene. The use of copper for graphene synthesis came quite late compared to other catalysts. The solubility of carbon in the copper is very low and the mobility of carbon can be described as a solely surface-based process [7]. The hydrogen atoms from methane are let out of the chamber as H_2 gas flow.
The production of graphene with CVD has a huge advantage which is the absence of heterogeneous materials. Compared to CNTs that consist of carbon-containing gases with metallic nanoparticles as catalyst[8]. The CVD grown graphene is preferable as one of the more pure forms for developing electrodes for sensors and the cost of production of pure graphene is becoming lower than other materials.[9] In recent works, CVD grown graphene is a preferable choice for scalable production because it generates large-area graphene layers. However, compared with mechanically ex-

foliated graphene the mobility may be lower and the transfer process can damage graphene and contaminate it with impurities [10].

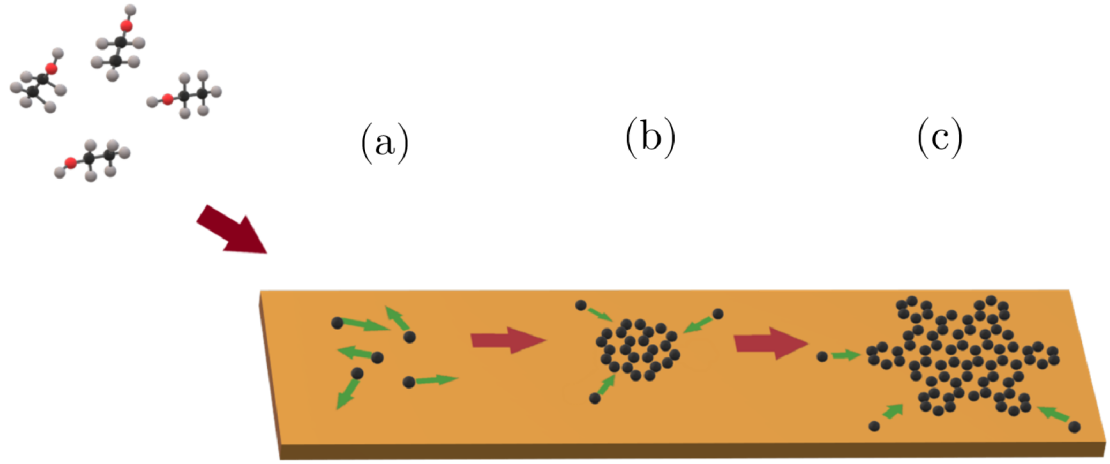

Fig. 1.4: Process of CVD growth: (a) catalytic decomposition, (b)nucleation and (c) expansion.

1.2 Electrochemical sensors

Some of the reasons why graphene is popular in applications of sensors, especially electrochemical sensors are wide range of electrochemical potential, fast electron transfer rate and high redox peaks with linear cathodic and anodic currents. Because of fast electron transfer graphene-based electrochemical sensing can detect smaller biomolecules like uric acid, ascorbic acid and dopamine [6]. When using graphene for biosensing two important factors are evaluated: the Debye length and suitable functionalization of the receptor with a single layer of graphene for detection of the specific molecules . When it comes to using graphene for electrochemical sensors, there are few main qualities making it a preferable choice. Firstly, the high surface area containing more active sites compared to other materials used for electrodes. Secondly, the possibility of electrochemical modification enabling covalent and non-covalent functionalization of the graphene.

1.2.1 Functionalization of graphene

To use graphene for biosensing applications it is necessary to properly functionalize graphene with components that bring detected molecules to its surface. Mainly, there are two ways of graphene functionalization, covalent and non-covalent methods. During the covalent method, the functional groups are introduced steadily and specifically. However, they convert the sp^2 carbon atoms of graphene to sp^3, changing graphene's physical properties and native electronic structure. On the other hand, the non-covalent strategy allows for a modification of graphene in a way that allows for the preservation of its inherent properties. Thanks to the strong affinity between graphene and aromatic molecules like pyrene, it is possible for them to stack across the graphene's basal plane via $\pi - \pi$ stacking. $\pi - \pi$ stacking interactions are attractive and nondestructive noncovalent interaction and are widely used for their strong binding force, nondestructive fabrication process and simple operation. $\pi - \pi$ stacking occurs between aromatic ring because they contain π bonds [11].

1-pyrenebutanoic acid succinimidyl ester or PSE is a linker molecule containing an aromatic ring and a reactive tail (see figure 1.5), which acts as an anchor for the recognition elements such as an enzyme or antibody upon their introduction to graphene's surface. PSE contains a pyrene group that stacks with graphene by π-π overlap and an N-hydroxysuccinimide (NHS) ester that reacts with primary amines [12]. Because of its electron-withdrawing behavior, PSE can cause a p-doping effect.

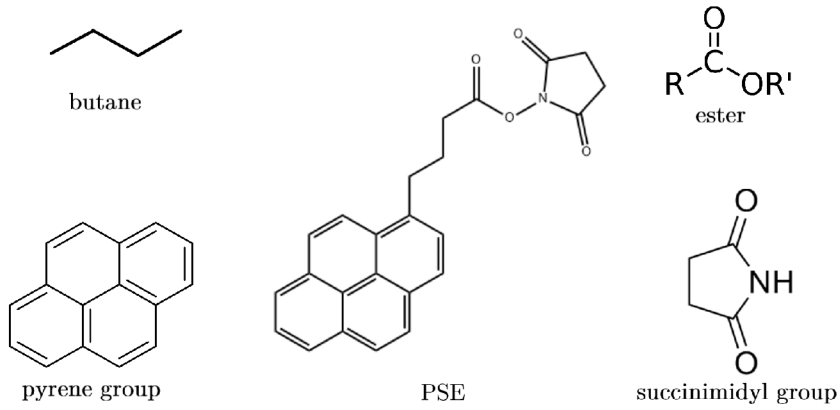

Fig. 1.5: 1-pyrene butanoic acid succinimidyl ester with its components.

Dimethylformamide or DMF is the best solvent for pyrene and its derivatives thus it is highly used during functionalization. The lone pair of electrons in the nitrogen atom in DMF causes electron transfer from DMF to graphene. This can result in the n-doping of graphene.

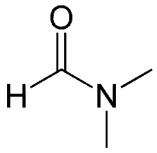

Fig. 1.6: Dimethylformamide.

Glucose oxidase or GOx is a part of the oxidoreductase family, which are enzymes that catalyze the electron transfer from oxidizing agents to reducing ones [13]. GOx is immobilized on graphene surface via an amide bond between the amino group of the enzyme and PSE. GOx which is a flavoprotein acting as a catalyst for the oxidation of beta-D-glucose at its first hydroxyl group, using molecular oxygen as the electron acceptor for the production of D-glucono-delta-lactone and hydrogen peroxide [14]. Both products of this reaction are responsible for the decrease in GOx activity. The presence of gluconic acid, which is a product of D-gluconolactone degradation, lowers the pH of the solution. Combination with the increase in H_2O_2 concentration can inhibit GOx activity [13]. GOx is a homodimeric enzyme with a flavin adenine dinucleotide molecule tightly bound to the active sites of every 80 kDa[1] subunit. After the catalyzation of converting glucose to glucono-D-lactone,

[1] 1 Da= $1.66 \times 10^{-}27\,kg$

the product is dehydrated and hydrogen/electron transfers to form $FADH_2$. This results in H_2O_2 production which leads to the inactivation of the GOx. The GOx activity is initiated by high levels of glucose in a medium with a pH of 4 to 6. The enzyme retains its stability at 40 °C for about 2 hours but loses its activity at temperatures above 50 °C. GOx is extracted from the fungus Aspergillus niger, which is the most used source of GOx for glucose monitoring and other industrial applications. This is thanks to a specific property of A. niger-derived GOx which is its very high substrate specificity for glucose binding [14]. The most suitable substrate for GOx is the D-glucose-β-anomer [13].

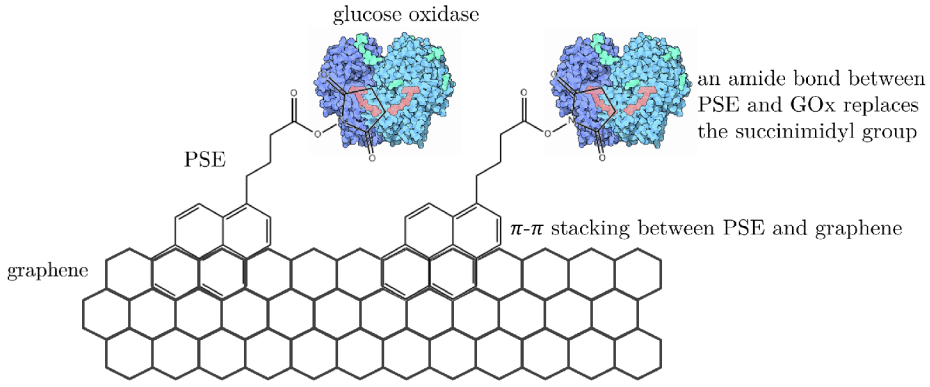

Fig. 1.7: Functionalization process.

Glucose is one of the most important compounds needed for life. It is fuel for glycolysis, downstream pathway of aerobic and anaerobic respiration. Glucose is produced from water and carbon dioxide through photosynthesis and condensed to form a starch. Glucose is an aldosic monosaccharide and contains six carbon atoms and an aldehyde group, which makes it an aldohexose. It can usually be found in two isomeric structures, dextrose-(D) glucose and lactose-(L) glucose. D-glucose is a naturally occurring form of glucose. Based on the orientation of hydroxyl (-OH) group attached to the first carbon atom, two more isomers are differentiated, i.e. alpha and beta glucose.

Phosphate-buffered saline or PBS is a buffer solution with pH of about 7.4. This water-based salt solution contains disodium hydrogen phosphate and sodium chloride. In GFETs when targeting physiological samples (for example blood) saline buffer like 1xPBS are used because of their short λ_D (explained below). Studies show that the lower the concentration of the PBS buffer solutions the higher the detection sensitivity. As the most successful concentration of PBS are 1x, or diluted at 0.1x or

0.01x, as they are close to biological conditions and lower salinity allows for longer screening distance. The Debye length in 1xPBS buffer is about ~ 0.7 nm so when using specific probe molecules the whole Debye length must be considered, because of the response signal screening [10]. Too long and the signal will be reduced.

1.2.2 Characterization of functionalization

Atomic force microscope

The atomic force microscope belongs to a scanning probe microscope techniques (SPMs). As the name suggests SPM technique is based on using a very sharp probe. The probe is scanning across the sample surface located as close as 0.1-100 nm and by recording various physical interactions creates a high-resolution image of the sample surface. Compared to electron microscope techniques one of the advantages of AFM is its ability to measure in air or fluid without the need for a high vacuum. Forces measured between the sample and the probe by AFM differ based on the situation, for example it can be a Van der Waals force, electrostatic force, chemical bonding, etc. The AFM consists of the probe connected to the end of a flexible microcantilever arm. This probe scans the surface of interest and the deflection of the cantilever arm is observed. Thus a three-dimensional picture of the surface can be reconstructed with high accuracy. Based on the type of sample and information aimed for in the measurement slight changes can be done in the measurement process. In contact mode, the probe is in constant contact with the surface and the signal corresponds to the cantilever bending. Whereas in dynamic modes the cantilever is oscillating at its resonance frequency. Depending on the interaction between the probe and the sample there is a shift in oscillations, on which the topography data are reconstructed. Cantilevers are usually rectangular or V-shaped and their top is coated with a thin reflective layer of gold or aluminium. The probe is a square-based pyramid or cylindrical cone made out of silicon or silicon nitride. The sample is positioned into or out of contact with the probe by the piezocrystal scanner. The scanner moves the cantilever or the sample. As for the detection of the cantilever bending, a beam of laser light is reflected from the top of the cantilever to the photodetector[15].

Raman spectroscopy

Raman spectroscopy is a part of vibrational spectroscopy based on the Raman effect. Raman effect occurs when monochormatic light strikes matter and part of the emitted light has a different wavelength. Unlike the Rayleigh scattering where the scattered light remains the same, the Raman effect changes the wavelength due

to inelastic scattering processes. Two types of scattering can be differentiated, the Stokes and Anti-Stokes. The main difference between them is that Stokes has longer wavelength than the exciting radiation. When atoms or molecules are already in an excited state Anti-Stokes scattering appears. They are usually caused by molecular vibration. By measuring the change in wavelength and interpreting it, information about the sample can be collected. Raman spectroscopy relies on laser as source of monochromatic light. The laser irradiates the sample and scattered light is examined with a spectrograph. The Raman spectrum of certain material contains its characteristic peaks[16].

1.3 GFET

The field-effect transistor is a type of electronic device with three or more terminals. The conductivity between two terminals can be modulated by the other one. The electric field created by the gate terminal determines the conductivity between the source and drain terminals. FET can be used as a switch since the gate terminal controls source-drain on/off current switching which is determined by the current magnitude. Control of the gate is achieved by modulation of free charge carrier density in the source and drain channel [17]. The application of gate electric field shifts the Fermi level related to Dirac point, by this way, the Dirac fermions of graphene can be transformed from electron to hole and vice versa. The concentration of charge carriers in graphene channel linearly depends on gate voltage :

$$n_{e,b} = \alpha V_G, \tag{1.2}$$

where n_e is electrom surface concentration, n_b is hole concentration, α is charge injection rate of the gate and V_G is gate voltage. The type of charge carriers is controlled by the polarity of gate voltage, in case of positive gate voltage the majority charge carriers are electrons, in case of negative gate voltage, the majority charge carriers are holes. The concentration of electrons and holes determine the graphene resistivity ρ that can usually vary in range from hundreds to thousands and can be expressed as [18].

Resistivity:

$$\frac{1}{\rho} = en\mu, \tag{1.3}$$

where the μ is the mobility and concentration of charge carriers controlled by gate voltage according to relation 1.2.

Related to gate electrode, we can distinguish three possible configuration: back-, top- and dual-gated GFET.

Back-gated GFETs typically use the CVD grown graphene and Si with a layer of SiO_2 as substrate. Electrode patterns are created by optical or other lithography technique. Concentration of carriers in this configuration can be calculated as :

$$n = \frac{CV_G}{e} \tag{1.4}$$

where V_G is the applied gate voltage, q is the charge and n is the number of majority of charge carriers. C is the unit capacitance and defined as $C = \frac{\epsilon_r \epsilon_0}{d}$ and the d is the thickness of the dielectric.

Top-gated GFETs, usually some kind of insulator is selected as a gate dielectric and prepared on top of the graphene surface. For the insulator electrolytic solution is generally chosen. The graphene device is assembled by the use of a metal electrode

on the surface of the gate dielectric. The conductance of the graphene channel is modulated when the potential applied to the dielectric is changed. The solution-gated G-FETs have a smaller electrostatic double layer characterised by Debeye length (about 3 nm), compared to the oxide in back-gated FETs (approximatelly 300 nm). The electrostatic double layer in solution-gated GFETs forms between the interface of the solution and graphene [19].

Back- and Top-Dual gated GFETs are a combination of both previously mentioned arrangements, back-solid and top-liquid gate [18].The GFETs became a popular choice mainly because of properties such as tunable bandgap, ambipolar behaviour, large detection area, high sensitivity to the change of electrical environment, and ease of effective functionalization. With their detection mechanism being not only field effect, but also the doping and scattering effects. Vacancy-type defects of graphene are useful for functionalization because they can easily attach to carboxyl, hydroxyl, or other groups. Fermi energy can be changed due to the doping by substitutional impurities [20].

1.3.1 Electrical measurements and metrics

As mentioned before the general principle of GFET is based upon the change of charge carriers in the channel induced by modulation of the electrostatic field. Graphene makes for a beneficial channel material, because it is able to capture biological analytes near its surface. This alteration of the channel's environment caused by physical or chemical changes can be detected by its electrical metrics. Generally, for the characterization of the FET's qualities two different measurements are utiliesed:

- transfer curve
- time series

Transfer curves

Transfer curves are obtained by changing the gate voltage V_G while the the voltage between the drain and source electrodes V_{DS} is a fixed bias. Usually the outcome of this approach is I_{DS} (or resistance $R_{DS} = V_{DS}/I_{DS}$) as a function of the gate bias. This results in a V-shaped curve with the minimum represented by charge neutrality point (CNP). CNP also known as Dirac point is where the populations of positive and negative charge carriers are equal. The left branch represents p-branch where the positive charge carriers are dominant and the n-branch on the right side of the CNP with the majority of charge carriers being electrons. The transconductance is

the linear extension of the branches from the CNP :

$$g_m = \frac{I_{DS}}{(V_G - V_{DP})} = \frac{W}{L}\mu C_G V_{DS} \tag{1.5}$$

where the V_{DP} is the voltage at the CNP, W the width and L the length of the graphene, μ the mobility of charge carriers and C_G the capacitance of the gate. In the back-gate configuration the C_G is inversely proportional to thickness of the insulating layer t:

$$C_G \propto \epsilon_r / t \tag{1.6}$$

the ϵ_r is the permeability of the dielectric. For the top-gate configuration the capacitance mainly depends on the electrical double layer formed between the graphene surface and electrolyte. The top-gate capacitance is much bigger compared with the back-gate capacitance so the gate potentials applied to top-gate are more efficient. The sweep gate voltage ranges in $\pm 1\,\mathrm{V}$ for top-gate configuration while for the back-gate it is $\pm 100\,\mathrm{V}$. The back-gate configuration is then much more applicable for volatile analytes in gaseous media rather than for biological samples. The capture of biomolecular analytes happens during the immersion of the probe to analyte-enriched buffer on functionalized graphene layer.

The voltage of the **charge neutrality point** is based on the doping level of the graphene. In intrinsic graphene the V_{DP} is close to $0\,\mathrm{V}$. However, the real graphene can be either n-doped or p-doped depending on the purity of graphene, materials of electrodes, substrate and media. Also the level of doping can be caused by the production process of graphene. In biosensing the measurements of V_{DP} can be done regardless of the graphene doping state of the graphene. The interaction of biological targets and recognition elements causes alteration of the doping level of graphene causing shift of the CNP voltage. The polarity is the shift of CNP towards negative(positive) voltage as p-doping (n-doping) and depends on the interactions between functionalized graphene layer and analyte molecules. For glucose it was reported to be measured both p- and n-doping, the inconsistencies were not further investigated in literature [10].

Another important metric is **transconductance** which is the ability to convert small change in the voltage to large change in current. The transconductance is dependent on the mobility of charge carriers μ which is an indicator of structural and electronic qualities.

The last metric describing transfer curves is the change in the amplitude of the electrical **current** in the p-/n-branches or in the Dirac point. The change of electrical current:

$$I = qnv \tag{1.7}$$

indicates the change in the carrier concentration or scattering processes. It can happen that the lateral shift of CNP causes modification in charge carrier density and on the other hand the decrease of the transconductance reflects scattering. Thus when measuring the change of current at given voltage it is difficult to figure out contributions from the two mechanisms.

Time series

Time series is captured by measuring the drain-source current as a function of time upon introduction of the reagents and continues during the reaction between analyte and sensor. The gate voltage and drain-source voltage remain fixed. With the fixed gate voltage representing a single point of transfer curve. The amplitude and the polarity of the signal is directly impacted by the value of fixed voltage. However, the current change in time series cannot be attributed to a specific mechanism. To avoid complications and limitations of time series a two-dimensional plot can offer a better insight. It is obtained by oscillating gate voltage. Preferably, the gate voltage is somewhere around the Dirac point. The electrical current is then plotted as a function of both time and gate voltage.

When comparing some type of metric, the **measurement before and after** exposure can provide some kind of quantitation of an analyte. Recording specific time point can reveal doping level. For example by observing the Dirac point of a transfer curve. Also to verify functionalization or the linking of the target. Most frequently used in detection of different analytes as ions, DNA, proteins and glucose. Output curves can also be used. However, the post-processing is needed because obtaining metrics like transconductance and CNP requires adequate voltage sweep. In before and after measurements the incubation time is usually very long so it is guaranteed that the reaction really happened.

Real-time measurements covering longer time intervals allows for observation of the removal unbound analytes, dissociation of the analyte and also for quantitation purposes. Real time measurements are essential in monitoring reaction rate and the stabilization process of the interaction. This type of information can help in timing of transfer curve measurement. Time series measure current at fixed biases discribes the kinetics of the interactions between analyte and sensor, but gives little information about their mechanism. Quantitative investigations based on current

changes only work if the change in graphene doping state is proportional to current, so the p/n breanches are in the linear regime.

1.3.2 Parameters of GFET biosensors

Quite a few properties of GFETs biosensors can be assessed but there are four main criteria in terms of quality which can evaluate their performance.

Spatial range of detection

Charged molecules in electrolyte of the GFETs are detected by counter-ions. Their electric potential is decreased exponentially with the Debye length:

$$\lambda_D = \sqrt{\frac{\epsilon k_B T}{2 N_A e^2 I}} \tag{1.8}$$

where ϵ is the permitivity of the solution, k_B the Boltzmann constant, T the temperature, N_A is the Avogadro's number, e is the charge of the electron and I is ionic strength of the medium. Ionic strength is a function of the concentrations of all ions in the solution $I = \frac{1}{2}\sum_{i=1}^{n} c_i z_i^2$, one half because both cations and ions are included, c_i is the molar concentration of ion i and z_i is the charge number of ion i [10]. The Debye length can be thought of as the distance with which the charges are detected. Consequently the charges with the Debye length larger are not detectable by the sensor. The Debye length at room temperature in aqueous solution becomes $\lambda_D(nm) = \frac{0{,}304}{\sqrt{I}}$. Restrictions caused by the Debye length can be eliminated by covering graphene with polymere permeable to biomolecules or by creating fixed-ion region with macromolecules.

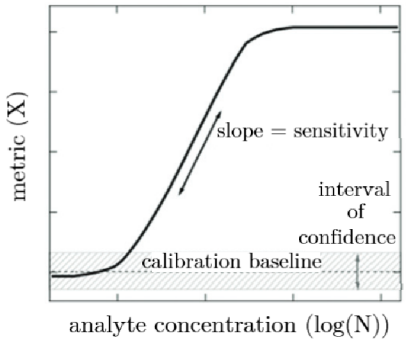

Fig. 1.8: LOD and sensitivity. Reproduced from [10]

Limit of detection

Limit of detection (LOD) is the smallest amount of analyte's concentration which can be detected by the sensor. To find out LOD couple of methods are used. Most used are extrapolation and direct measurement. The sensor baseline should be defined for both methods for example via standard deviation of the electrical metric.

Sensitivity to target concentration

Sensitivity of the system is defined as the slope of linear regime of the curve:

$$S = \frac{\Delta M}{\Delta N} \tag{1.9}$$

ΔM represents change in observed electrical metric and its corresponding change ΔN in the concentration of the analyte. Sensitivity can be measured experimantaly by comparing the Dirac point and transfer curves in before and after measurements.

Response time

It is important to determine time needed to obtain result from the sensor for given application. Signal stabilization after the introduction of the sample or after its removal and changing of the electric potentials play role in determining the response time. It can also thought of as the reach of a current saturation necessary to find out the incubation time of the target.

2 Literature retrieval

The goal of this literature retrieval is to compare current methods of graphene functionalization suitable for biosensing of glucose and showcase current processes for the detection of biochemical compounds. The search for a convenient self-measurement device detecting glucose in the body has great importance for diabetics to monitor their condition properly in time. Graphene based biosensors show incredible possibilities in modern biosensor development with unique properties like large detection area and effective functionalization.

2.1 Graphene compared with SWNTs

In 2010 Huang et al. [22] showed the utilization of large-sized CVD grown graphene as a part of a field-effect transistor for biosensing of glucose and glutamate molecules in real-time. Compared to single-walled carbon nanotubes (SWNTs), which are carbon sheets rotated into cylindrical tubes 1-2 nm in diameters, graphene exhibits many advantages in terms of biosensing devices. SWNTs are difficult to manipulate for device fabrication, hard to distinguish between metallic and semiconducting nanotubes and too small to connect with large-sized bio-species, thus complicated to be bio-functionalized. CVD grown graphene has great potential to become an alternative to SWNTs. The CVD grown graphene was transferred from Ni film to SiO_2/Si by etching away the Ni with HCl. The PMMA which was spin-coated on the graphene during the growing process was removed with acetone after the transfer to SiO_2/Si substrate and annealed at 450 °C. Such device was then immersed in a 5 mM linker molecule (1-pyrenebutanoic acid succinimidyl ester) in DMF for 2 h at room temperature, rinsed with DMF and DI water. The device was then introduced to a drop of 10mg/mL GOx or 2mg/mL of glutamic dehydrogenase (GluD) in $Na_2CO_3 - NaHCO_3$ buffer solution overnight at 4 °C. Rinsed again with DI water and PBS, and submerged in 0.1 M ethanolamine solution for half an hour to remove unwanted remaining reactive groups.

The authors also showed that the GFETs functionalized with GOx did not respond to glutamate L-ascorbic acid, uric acid and acetaminophen. Implying that this kind of graphene biosensor can specifically detect glucose. Catalytic oxidation of glucose and glutamate caused an increase in graphene conductance. The transfer curves with I_{DS}-time measurement confirmed the increase in the device conductance. Right shift of the transfer curve can be observed after the introduction of glutamate, which is a sign of the p-doping effect. The shift to the right is only minor for glucose, explaining lower detection sensitivity. It is possible that the products

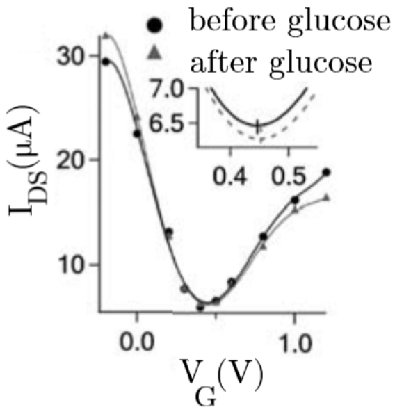

Fig. 2.1: Transfer curves before and after adding glucose, reproduced from [22]

from the oxidative reaction, H_2O_2 and NH_4OH, induce an increase in graphene conductance. The GFETs exhibited a detection limit of 0.1 mM for glucose and 5 µM for glutamate.

2.2 Transfer-free CVD graphene for glucose sensing

CVD grown graphene shows great potential in biosensing applications. However, typical metal-based CVD graphene is contaminated with polymer transfer-support and heavy metal ions. Wei et al. [23] in 2020 grew few-layer graphene directly on SiO_2/Si substrate without a transfer process and used it to develop a glucose sensor. To reduce the difficulties of GOx immobilization on the surface of intrinsic CVD graphene, the graphene is functionalized with oxygen plasma to improve hydrophilicity. Formed oxygen-containing groups on graphene increase the effectiveness of GOx immobilization. Subsequently, the Nafion layer is deposited on the surface functionalized by oxygen plasma treatment and acts as the protective film. The CVD was grown in a quartz tube reactor inside a horizontal CVD furnace at atmospheric pressure. Before the samples of SiO_2/Si were loaded into the tube they were washed with deionized water, acetone and isopropanol. The tube was flushed with argon and heated to growth temperature. Followed by injecting H_2 and CH_4 as $H_2/CH_4 = 75/17.5$ sccm at 1100 °C for 2 h. Then the G/SiO_2/Si was bonded to the copper wire with conductive silver paint. Oxygen plasma with a power of 40 W under the pressure of 0.3 mbar and 5 scccm oxygen flow. The oxygen treated plasma graphene on the SiO_2/Si substrate was used as the working electrode. The drop of

10 µL GOx solution was dried on the electrode for 1 h at room temperature followed by a thin Nafion layer.
AFM characterization shows that the surface roughness of OPG is reduced. XPS was used to evaluate the effect of plasma treatment on the chemical composition of $G/SiO_2/Si$. 17 % of C-O and O-C=O peaks are present compared to pristine graphene. This type of OPG can facilitate the immobilization of enzymes because of carboxyl bonding with the amino group of the GOx enzyme. The biosensor produced as described, for electrode surface area of 0.25 cm^2, shows a sensitivity of 16.16 $\mu A m m^{-1} cm^{-2}$. The LOD is estimated to be 124.19 µM (S/N=3), which among other glucose biosensors is relatively high. This transfer- and metal-free process of sensor fabrication shows significant advantages. Mainly eliminating residues such as PMMA, which severely retards the electron transfer and degrades electrochemical activity.

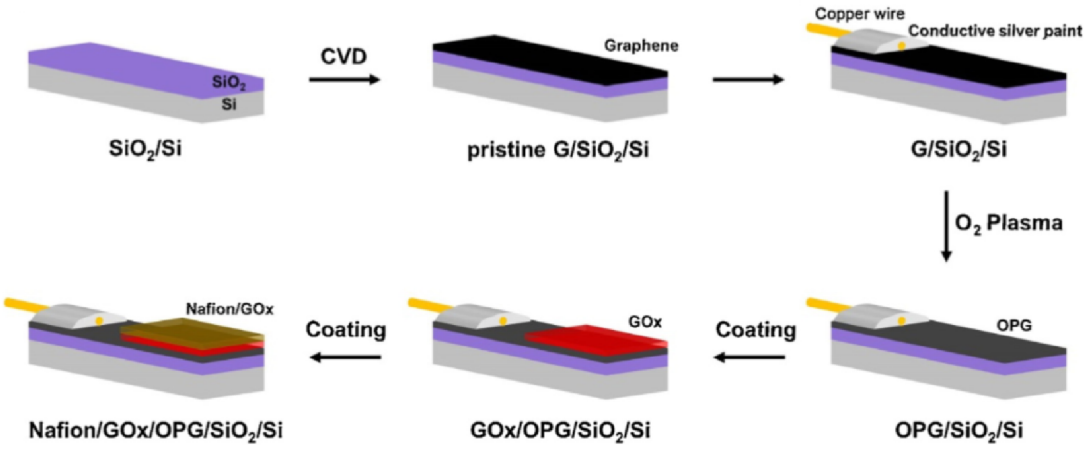

Fig. 2.2: Schematic fabrication process of the graphene sensor. Reproduced from [23].

2.3 On-site detection of glucose

In 2022 Huang et al. [24] created a fully integrated graphene-polymer field-effect transistor device for on-site detection of glucose in human urine. Through the shadow mask, gold vapour was attached to the substrate. After the single-layer graphene was transferred to the substrate.
Different compositions of poly(acrylamide (Aam)-3-acryl-amidophenylboronic acid (AAPBA)- N-dimethylaminopropylacrylamide (DMAAPA)) were introduced to the sample and immobilized on the sensor through a $\pi - \pi$ bonding between the AAPBA and graphene. The AAPBA in the synthesized polymer acts as the receptor. The

GFET was then immersed in polymer solutions in DMF for 3 h. Graphene is utilized as a conductive channel and functionalized with polymer. The physisorption interaction between AAPBA and any other components of urine is much weaker than the chemisorption between the AAPBA and glucose, which is supported by the density functional theory study. Furthermore, it was confirmed that the sensor can recover its detection capability after hydrochloric acid treatment because of the reversible reaction between the polymer and glucose. The covalent bonds between polymer and glucose can dissociate under an acidic environment. Thus making it reusable up to 20 times. The accuracy in response of reused sensors is about 86 % or up for different concentrations of glucose solutions. Different concentrations of glucose were obtained by measuring drain-source current I_{DS} or by the graphene transfer characteristics. Experimental data shows that the sensor holds high sensitivity of 822 $\mu A.cm^{-2}.mM^{-1}$ with a LOD of 1,9 μM while glucose monitoring human urine in a range of 0.04-10 mM. After the polymer treatment and with the introduction of the glucose solution, it was found that the Dirac point increased from -48.3 to -23.3 mV. AFM measurements showed an increase in graphene thickness after polymer functionalization by 8 nm-10 nm.

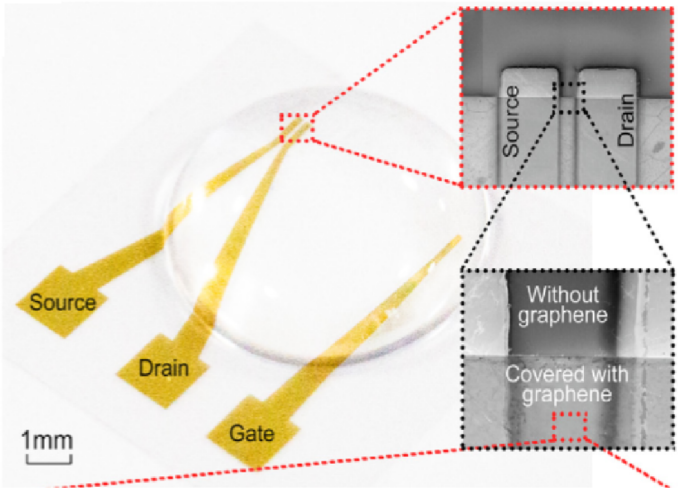

Fig. 2.3: Liquid-gated P-GFET, reproduced from [24].

3 Experimental part

3.1 Sensor fabrication

3.1.1 Preparation of the sensor

In order to prepare fully functioning graphene sensor for glucose detection, multiple step process was followed. First step was the preparation of the Cu foil with CVD grown graphene on both sides. The foil was annealed at 110 °C for 15 minutes to remove any excess water. This was followed with spincoating the PMMA onto the foil and left to dry for 24 hours. Reactive-ion etching with oxygen plasma was then used to remove unwanted graphene from the other side of the foil. The copper foil is etched away by the solution of iron(III) nitrate nonahydrate ($Fe(NO_3)_3.9H_2O$) for 2 hours. After that the layer of graphene with PMMA is four times rinsed with DI water and left to bathe for 5 minutes in 5 % HCl solution. The cleaning of the copper foil is finished after four times rinsing in DI water and ethanol. At this point graphene can be transferred onto the sample, dried with nitrogen and left to dry for 24 hours. It is recommended for the samples to be annealed for at least 45 minutes at 180 °C before the graphene transfer. To remove the layer of the PMMA the sample is immersed in acetone for 60 minutes and heated to 52 °C. Afterwards it is rinsed with IPA, ethanol and left to dry.

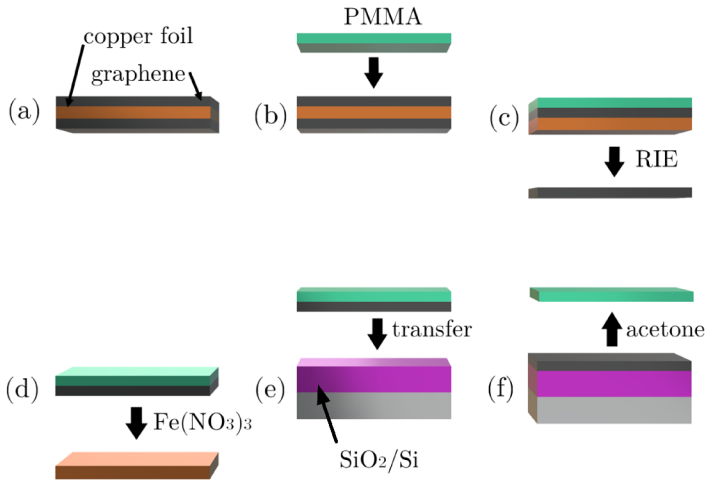

Fig. 3.1: Process of sample preparation.

As for the farbication process of the silicon wafer, with layer of SiO_2 and gold electrodes optical litography is used. Positive photoresist AZ 5214 E is spin-coated onto the silicon wafer and exposed to UV light. In the next step developer AZ 726 MIF is used. The sample is then covered with thin layer of Ti so the following Au layer sticks correctly to SiO_2. The unwanted gold layer is removed with the "lift-off" process.

3.1.2 Functionalization of the sensor

The functionalization process of graphene for glucose detection consists of two parts. In the first part the PSE linker molecules are attached to graphene surface via $\pi - \pi$ bonding. Next part is the immobilzation of GOx through amide bond with PSE linker molecules. In the first part silicon wafer with layer of SiO_2 and gold electrodes is immersed in the solution of 5 mM PSE linker molecules in DMF. The samples are covered in the solution 2.5 h at room temperature. After, the samples are rinsed twice with IPA and twice with DI water. For the next part the GOx in 1xPBS at concentration of 10 mG/mL was dropped onto the sample. The sample was refrigerated with moist paper underneath and fully covered to ensure the solution does not evaporate for 15 hours. The unreacted GOx was washed with 1xPBS and DI water.

3.1.3 Assembly of the sensor

After the first part of the functionalization process the sample with attached PSE molecules was glued to a glass plate. For the back-gate configuration silver paste and wire was used between the silicon wafer and glass as a connection to electrical circuit. The sample was then on both sides of the golden electrodes taped with Kapton tape as insolation. The electrodes were also contacted with silver paste and wires, the distance between the electrodes was 2.2 mm. GELPACK® barrier was created around the graphene flake. The GOx in 1xPBS was dropped onto the graphene flake and left in the fridge for 14 to 16 hours with water soaked paper to limit the evaporation of the solution. The assembly could not have been done before the PSE immobilization, because the DMF could dissolve any used plastic and adhesives.

3.2 Characterization

3.2.1 Characterization by AFM

AFM measurements were carried out on the surface of graphene to ensure the functionalization process was successful. The images were taken with Bruker Dimension Icon on the same spot of the sample using tapping mode. The area of scanning was 1.5 by 1.5 µm and captured the interface of graphene layer and SiO_2. Figure 3.2 (a) shows the sample before the functionalization. The height difference between the SiO_2 surface and graphene of ∼1 nm was obtained by averaging multiple scan lines of the length 0.9 µm, see figure 3.3 (a). Peaks above the monolayer can be caused by some kind of bending of the monolayer, impurities and PMMA residues.
Next figure 3.2 (b) was captured after the sample was immersed in 5 mM solution of PSE for 2 hours at room temperature and rinsed with IPA and DI water. As seen in this figure, the graphene layer evened out after the introduction of PSE solution. This suggests the PSE was evenly distributed and immobilized across the surface of graphene. The increase of height on the part of the sample with graphene was observed. The increase of ∼1 nm corresponds with [25]. Subsequently, drop of GOx solution was placed on the sample for 16 hours and refrigerated. Followed with rinsing in 1xPBS, DI water and air drying.

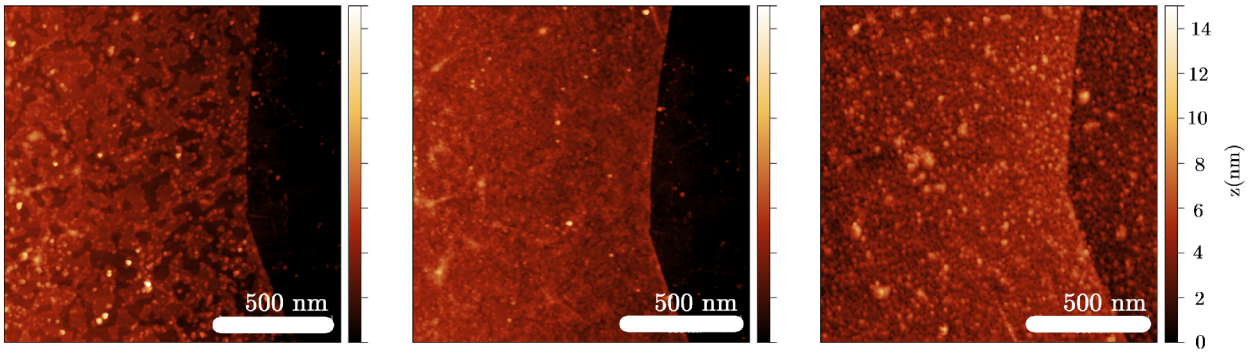

Fig. 3.2: AFM images of the sample before the functionalization process (a), after the introduction of PSE (b) and after the GOx immobilization(c).

A clear modification of the surface was visible after the immobilization of the enzyme. The peaks are spread evenly and majority of them being the same height. Some of the irregularities on the surface with diameter of ∼ 100 nm can be attributed to huge conglomerates formed by the enzyme, as the molecule of glucose oxidase is only 5 by 8 nm [26]. The enzyme was expected to be washed away from the SiO_2

surface. However, some residues formed nonspecific bonds, caused by van der Waals forces and resisted rinsing process [27]. Thus, the scan lines in figure 3.3 (c) did not offer a proper insight. The increase in height of the surface was uniform across the PSE covered graphene monolayer and SiO_2. The uniform layer is expected to be $\sim$5 nm in height because of the dimensions of GOx.

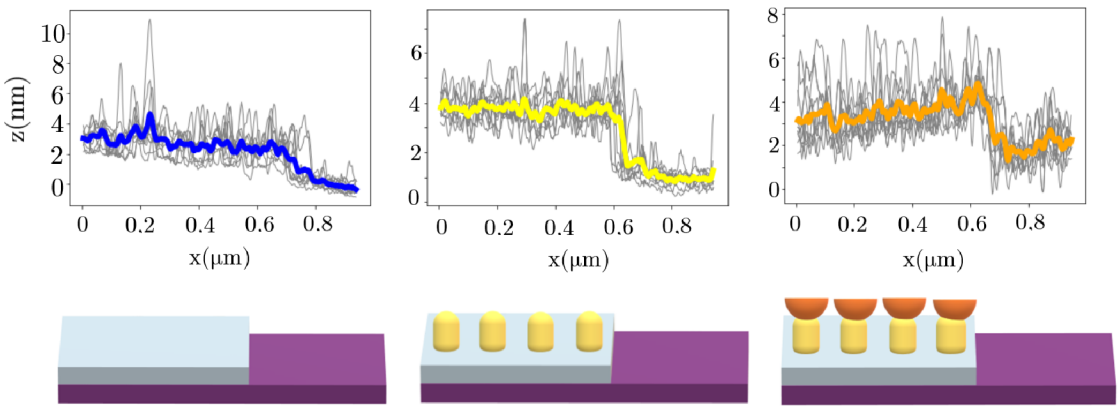

Fig. 3.3: Profile scan lines (up) of the functionalization process (down).

3.2.2 Characterization by Raman spectroscopy

When analysing the Raman spectrum of graphene there are few significant peaks. Three main peaks are to be considered, the G-band or graphite-band property of carbon-based material, the D-band indicator of disorders and 2D-band or second order harmonic band. The shift in G and 2D peaks represents doping effect on graphene. The intensity ratio I_{2D}/I_G can indicate if there are multiple layers of graphene. The Raman spectrum was obtained using Witec Alpha 300R with the laser 532 nm laser and power of the laser was set to 1 mW. First the measurements were done on the sample of graphene on SiO_2 surface, see figure 3.4.

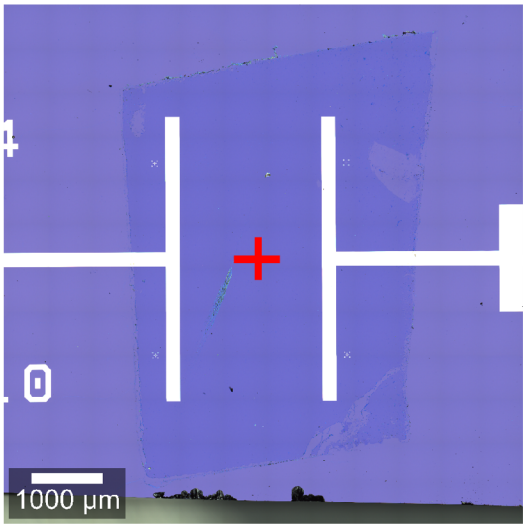

Fig. 3.4: Sample and point from which the Raman spectrum was obtained.

As seen in the figure 3.5 (a), graphene D peak is located at 1348 cm^{-1} with significant intensity, which indicates some defects caused by the graphene preparation or during annealing process. The G peak was measured to be at around 1598 cm^{-1} and 2D peak at 2688 cm^{-1}. The sample was then left for 2 hours in 5 mM solution of PSE in DMF, rinsed with IPA, DI water and left to dry. The values of the characteristic peaks were slightly shifted for D peak to 1341 cm^{-1}, G peak to 1590 cm^{-1} and 2D peak to 2682 cm^{-1}. It should also be considered that the sample was immersed in DMF, which can cause left shift of the G and 2D peaks. The DMF molecule contains N, thus it can cause doping effect. In figure 3.5 (b), new peak appears after the PSE functionalization process. Peak at 1627 cm^{-1} corresponds to the pyrene group resonance [28], which means the PSE was immobilized via $\pi - \pi$ stacking. However, the peak confirming attachment of the PSE at 1235 cm^{-1} was not observed [29]. This may be caused by the intensity increase around the D peak, which does not make it noticable. The PSE functionalization increases the disorder peak, because of the orbital hybridization of the PSE with graphene layer.

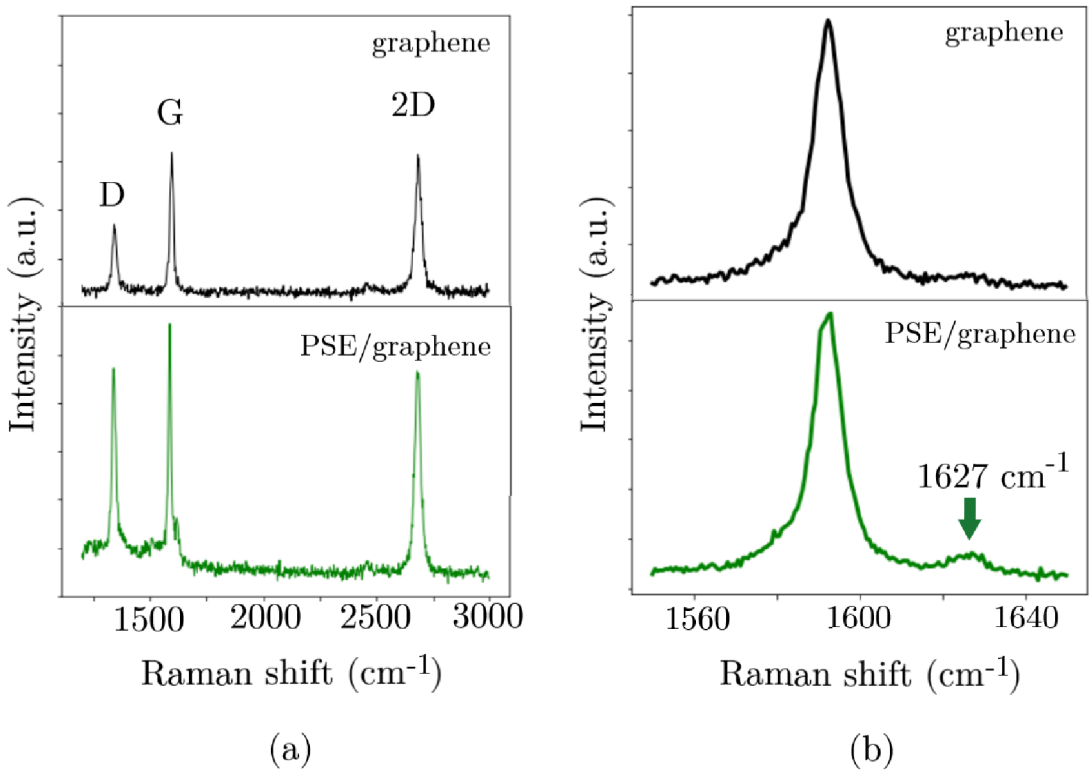

Fig. 3.5: Raman spectrum of untreated and treated graphene (a) and close-up of one of the peaks (b).

3.3 Measurements

After the functionalization process the sensor was ready for electrical measurements. The experimental setup as seen figure 3.6, was controlled with LabVIEW designed program. For measuring electrical characteristics lock-in amplifier Stanford Research SR830 was used with 10 MΩ resistor in series. For the gate voltage a Keithley 6221 AC/DC Current Source with parallel connection to 1 MΩ resistor was employed.

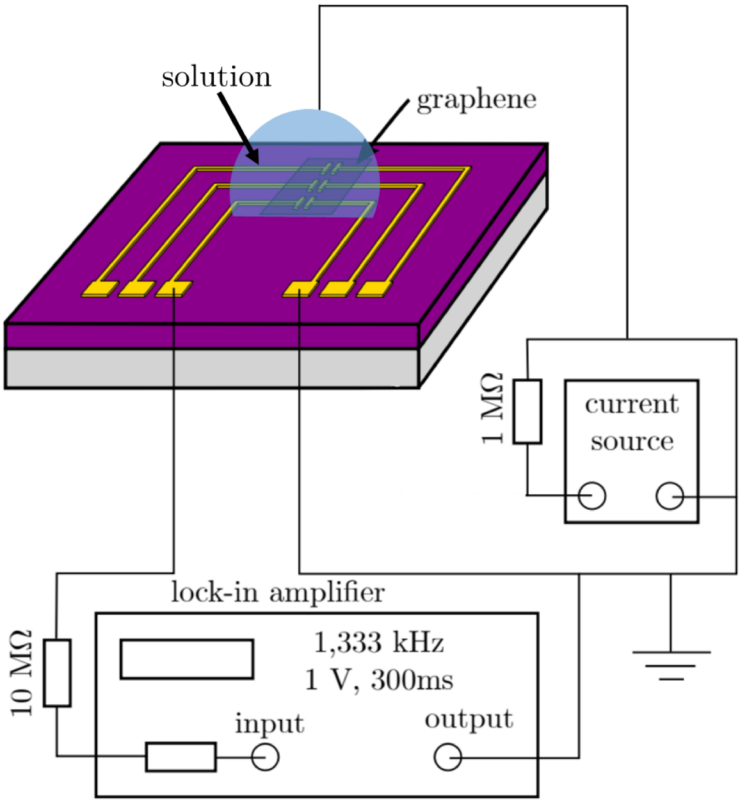

Fig. 3.6: Electrical circuit of the experimental setup for solution gated setup (reproduced from [31]).

The amplitude was set to 1 V for solution configuration and 75 V for the solid back-gate configuration. The time constant was 100 ms and frequency 1333 Hz. For the top-gate configuration gate voltage was applied with gold wire submerged into the solution. As a reference solution for measurements 0.01xPBS was used. The different concentrations of glucose were obtained by mixing D-(+)-glucose with 0.01xPBS.

3.3.1 Time response

The position of Dirac point via transfer curve was obtained with the value of V_{DP}= 0.23 V in top-gate configuration for the reference solution of 0.01xPBS (see figure 3.7 (a)). Then the applied gate voltages were set to constant values lower (figure 3.8) and higher (figure 3.9) than the voltage of Dirac point. The measurements in both figures represent real-time measurement of change in resistance due to the different concentrations of glucose. The solution with the lowest concentration was introduced to the sample and left to stabilize at 0 s. After every about 100 s the solution was cleaned of the surface with pipette and another one was added to the sample, causing rapid peaks in resistance. For the figure 3.8 where the gate voltage

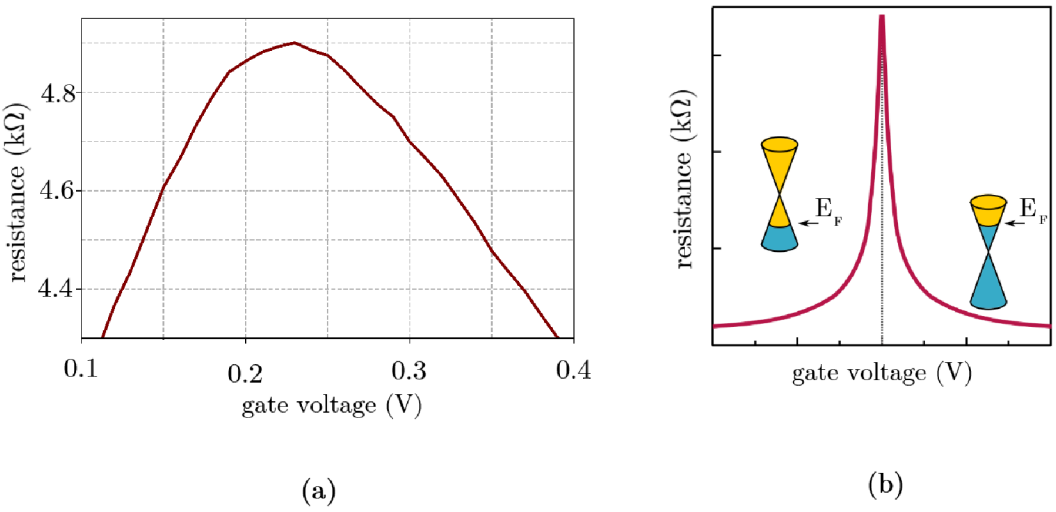

Fig. 3.7: (a) Transfer curve of the GFET with Dirac point at 0.23 V for a reference solution of 0.01xPBS, (b) ambipolar field effect in graphene (reproduced from [30]).

was 0 V throughout the whole time series, thus the measurements were done in p-doped region, see figure 3.7 (b). After the first stabilization of the concentration of 10 mM was changed for higher concentration the resistance has increased. However, for the concentrations 12 mM, 14 mM and 16 mM the change was not as obvious and sometimes even interchangeable. But the increase in the first half of the figure and decrease in the second is visible. For the n-doped region of graphene in figure 3.9 the measurements were first done for gradual increase of the concentration and difference in resistance for the concentrations of 16 mM, 23 mM, 28 mM and 32 mM is pretty obvious. In the part, where the concentration was decreased in smaller difference between the concentrations the decrease is again indistinguishable for the 14 mM, 12 mM and 10 mM solutions. Last concentration added to the sample was 8 mM and was left to stabilize.

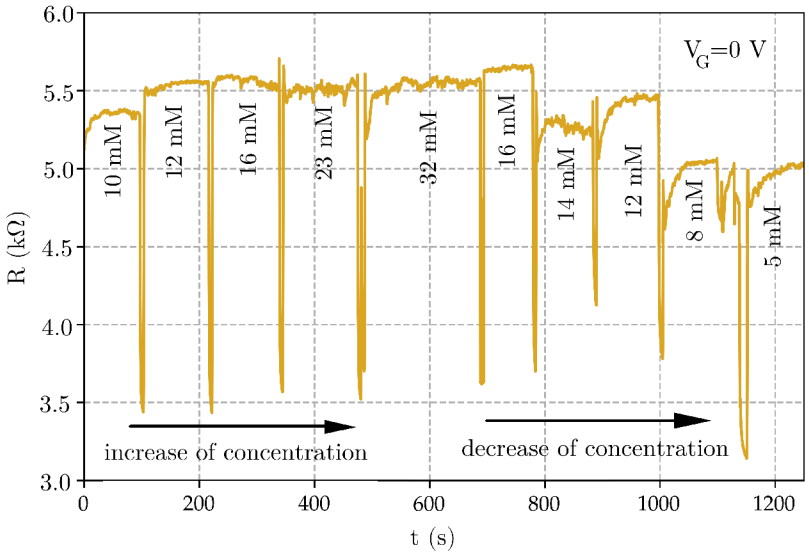

Fig. 3.8: Reaction in time to different concentration of glucose in top-gate configuration with the gate voltage of $V_G = 0\,V$, when $V_G < V_{DP}$.

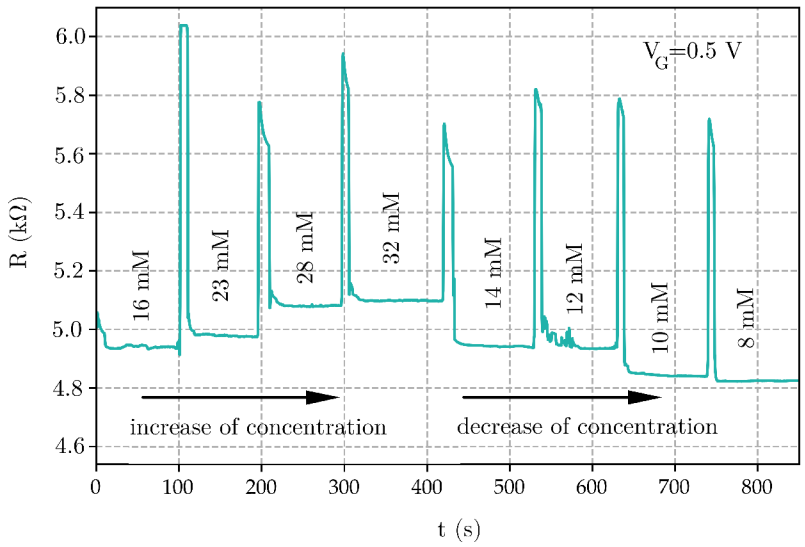

Fig. 3.9: Reaction in time to different concentration of glucose in top-gate configuration with the gate voltage of $V_G = 0.5\,V$, when $V_G > V_{DP}$.

3.3.2 Transfer curve

Top-gate

When measuring the transfer curves in the top-gate configuration of the sensor, the gate voltage was applied by immersing gold wire into the solution and amplitude was set to 1 V. The Dirac point was expected to be found in this interval. So the measurement was done by the sweep of gate voltage from 0 V to 1 V to -1 V back to 0 V by a step of 0.01 V every 0.5 s. The measurement exhibited a hysteresis characterized by the shift of Dirac point voltage (at maximum resistance) for increasing and decreasing voltage change (figure 3.10). The DP voltage was more positive for increase of voltage change and vice versa. The 0.01xPBS solution was used as a reference value during measurements and compared with various concentrations of glucose diluted in 0.01xPBS. In order to avoid the effect of hysteresis, the right Dirac point was typically compared, as it was more distinguishable. Some of the samples indicated initial n-doping in 0.01xPBS (see figure 3.10) and few p-doping (figure 3.14).

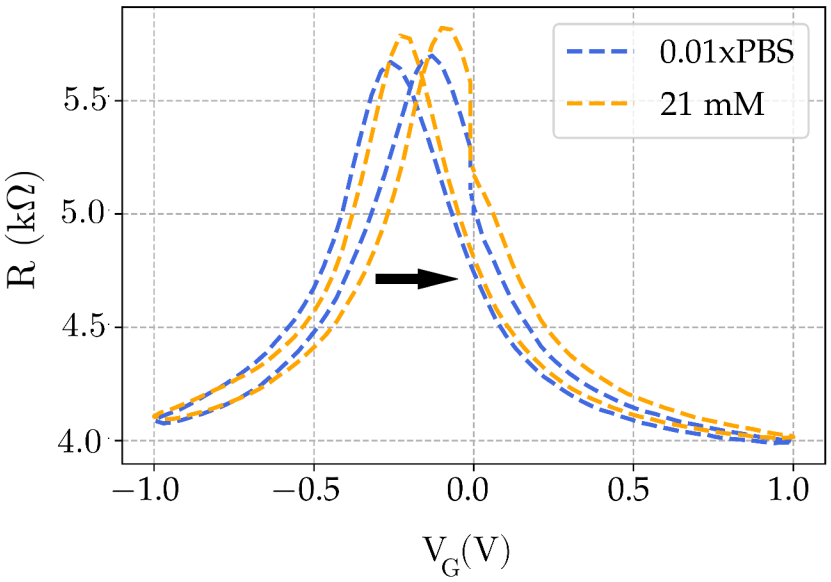

Fig. 3.10: Hysteresis of transfer curves and the shift of the curve for 0,01xPBS used as reference (blue) and 21 mM glucose solution (orange).

However the shift in Dirac point for different concentrations of glucose was always to the right from the reference value for 0.01xPBS indicating p-doping of graphene by glucose. The shift characterized by the difference between the Dirac point of reference solution and given concentration was observed for numerous concentrations,

as seen in figure 3.11. Each shift of Dirac point for given concentration was measured on different sensor. Nevertheless, it is clear that with higher concentration the shift increases. Figure 3.12 shows transfer curves for one sample, the reference value indicated initial n-doping.

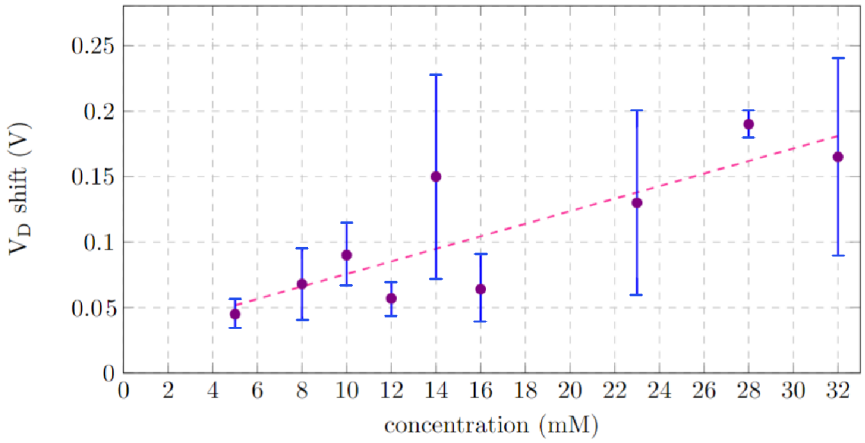

Fig. 3.11: Shift of Dirac point for various concentrations of glucose solution.

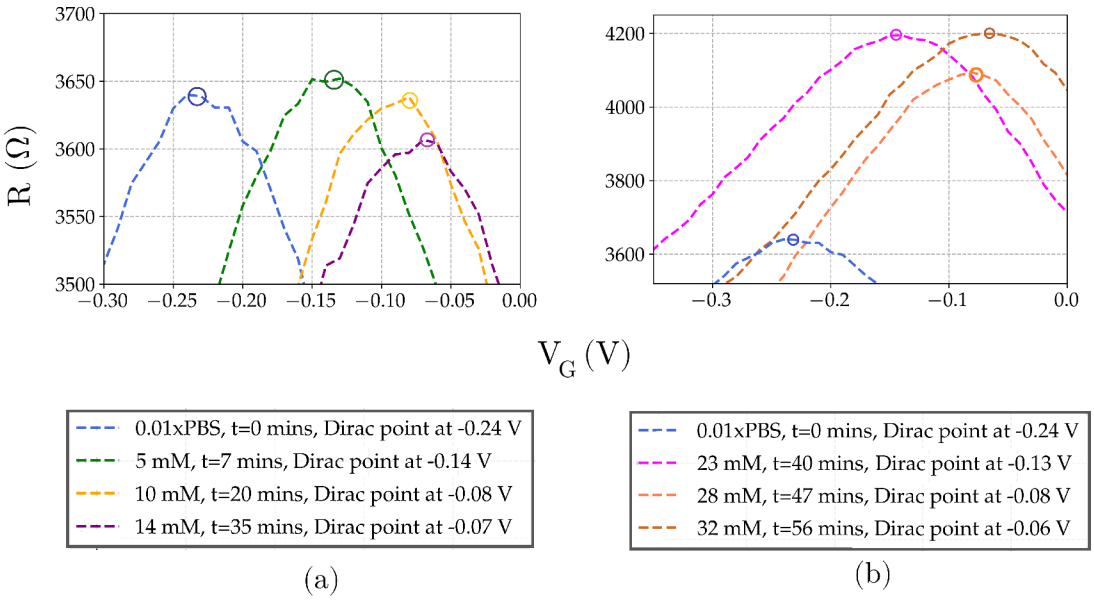

Fig. 3.12: Transfer curves with Dirac points (circles) for lower(a) and higher (b) concentrations and time of measurement.

Subsequent p-doping caused by glucose solution creates difference in Dirac point position from reference value in 0.1 V to 0.19 V. The increase in resistance in figure

3.12 (b) is mostly determined by the degradation of graphene. The shift of the Dirac point and the transfer curve was slightly varying in the time (see figure 3.13). The sensor is also sensitive to the time of usage.

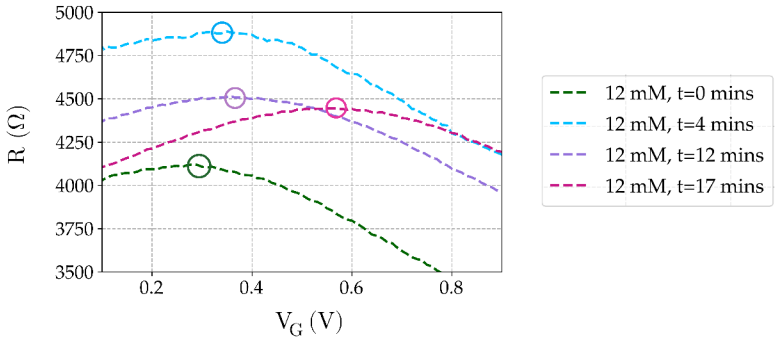

Fig. 3.13: The evolution of transfer curves for the same concentration measured in different times.

Back-gate

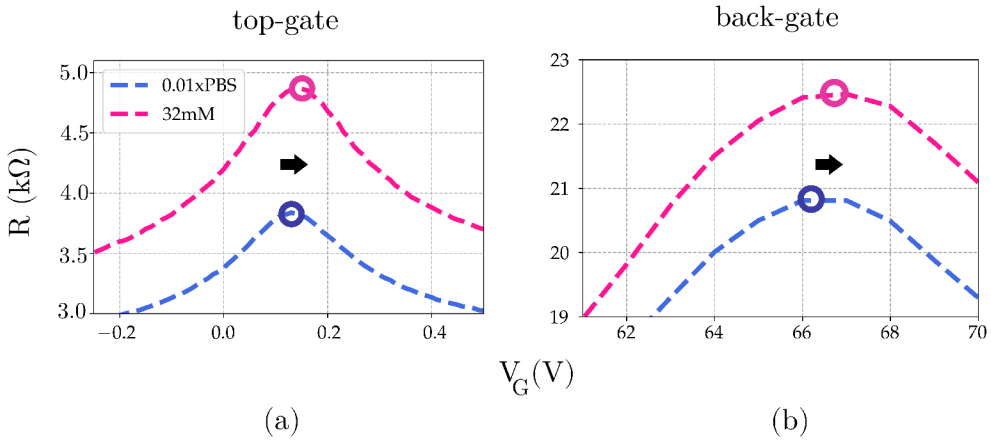

Fig. 3.14: The transfer curve for the reference solution of 0.01xPBS and glucose concentration of 32 mM for top-gate (a) and back-gate (b) configuration of the sensor.

The immersed gate configurations is preferred for direct electrical measurement in electrolytic solution, because of screening by the EDL can lessen the back-gate voltage [10]. Applied gate potentials can reach over two orders of magnitude for back-gate configuration in comparison to top-gate. An example of such comparison

can be seen in the figure 3.14 (a) the Dirac point was found at 0.14 V for reference solution and shifted to 0.16 V for the 32 mM concentration of glucose in the top-gate arrangement. The same experiment performed in the back-gate exhibited the Dirac point at 66 V for shifted to 67 V.

3.4 Results discussion

Graphene employed as a channel in field-effect transistor can be modified to selectively react to glucose. Functionalization process immobilizes PBS on the graphene surface via $\pi - \pi$ binding. In the next step of functionalization GOx replaces the succinimidyl group of PSE, thus binds with PSE through an amide bond. Raman spectroscopy verified the binding of PSE and further confirmation of proper functionalization was done by AFM. AFM images showed visible alteration of the surface after each step of the process.

Response of the sensor observed at fixed gate voltage in top-gate configuration shows increase in resistance with the growing concentration. Though, concentrations with the change smaller than 3 mM were not distinguishable in time response measurements.

Transfer curves for different concentration of glucose suggest that the PSE/GOx functionalized graphene is n-doped. The shift of the Dirac point was observed for the top-gate configuration in the interval of 0.03 V to 0.35 V. The displacement of the Dirac point can also be attributed to not only different concentration of glucose, but time at which the measurements were taken and the number of sensor usage. The back-gate configuration is much less efficient for electrolyte sensing with the applied gate voltages being significantly higher at around 66 V for Dirac point. The shift in Dirac point for concentration of 32 mM was +1 V.

Conclusion

The goal of this bachelor's thesis was to properly modify the surface of graphene in a way to selectively react to glucose. This was achieved with noncovalent functionalization with 1-pyrenebutanoic acid succinimidyl ester as linker molecules via $\pi - \pi$ bonding and subsequent immobilization of an enzyme glucose oxidase. Glucose oxidase shows high selectivity for glucose detection and is utilized as a recognition element of the sensor.

The functionalization process with PSE linker molecules was characterized by Raman spectroscopy. Both steps were evaluated by Atomic Force Microscopy. The surface was visible altered and can be assume that the process of immobilization was successful.

The response of the sensor was studied in a top-gate and back-gate configuration with transfer curves and real-time response. Both configurations of the sensor showed p-doping. However, the top-gate configuration of the sensor was more efficient. Real-time measurements indicated the sensitivity to a glucose concentration with the rise of resistance at fixed gate voltage. The shift of the Dirac point was observed for multiple concentration of glucose and increased with the rise of the glucose. It should also be considered that sensor response varies in sensitivity with the duration of the measurements.

The GFETs as a biosensor for glucose detection show great promise and good selectivity. The modified graphene can be easily fabricated into sensor. Further research needs to be done on reuseability and routine analysis of glucose in real blood samples.

Bibliography

[1] GEIM, A.K. and KONSTANTIN, S. The rise of graphene. *Nature Materials.* NATURE PUBLISHING GROUP, **2007**, vol. 6, p. 183 – 191, [cit. 2022-4-19]. ISSN 1476-1122. Available from: doi:10.1038/nmat1849.

[2] YANG G., LI L., LEE WB., et al. Structure of graphene and its disorders: a review. *Science and Technology of Advanced Materials* **2018**, vol. 19(1), p. 613 – 648 [cit. 2022-5-18]. ISSN 1468-6996. Available from: doi.org/10.1080/14686996.2018.1494493.

[3] PHAM, T. H. Graphene and its one-dimensional patterns: from basic properties towards applications. *Advances in Natural Sciences: Nanoscience and Nanotechnology.* **2010**, vol.1(3), p.033001 [cit. 2022-5-18]. ISSN 220436262.

[4] NETO C., GUINEA F., PERES N., et al. The electronic properties of graphene. *Reviews of Modern Physics.* **2009** vol. 81(1) p.109 – 162, [cit. 2022-5-18]. ISSN 1539-0756. Available from: doi.org/10.1103/RevModPhys.81.109

[5] GEIM, A.K. and KONSTANTIN, S. The rise of graphene. *Nature Materials.* NATURE PUBLISHING GROUP, **2007**, vol. 6, p. 183 – 191, [cit. 2022-4-19]. ISSN 1476-1122. Available from: doi:10.1038/nmat1849.

[6] NAG, A., MITRA A., MUKHOPADHYAY, S. C., et al. Graphene and its sensor-based applications: A review. *Sensors and Actuators A: Physical.* **2018**, vol. 270, p. 177 – 194 [cit. 2022-4-19]. ISSN 1530-6984. Available from: doi.org/10.1016/j.sna.2017.12.028.

[7] LI, X., CAI W., AN, J., et al. Large-Area Synthesis of High-Quality and Uniform Graphene Films on Copper Foils. *Science.* **2009**, vol. 324(5932), p. 1313 – 108 [cit. 2022-2-27]. ISSN 0379-6779. Available from: doi:10.1126/science.1171245.

[8] PUMERA, M. Electrochemistry of graphene: new horizons for sensing and energy storage. *The Chemical Record.* **2009**, vol.9(4), p.211 – 223 [cit. 2022-5-18]. ISSN 1528-0691. Available from: doi.org/10.1002/tcr.200900008.

[9] PUMERA, M., AMBROSI, A., BONANNI, A., et al. Graphene for electrochemical sensing and biosensing. *TrAC Trends in Analytical Chemistry.* **2010**, vol.29(9), p.954 – 956 [cit. 2022-5-18]. ISSN 1659936. Available from: doi.org/10.1016/j.trac.2010.05.011.

[10] BÉRAUD, A., SAUVAGE, M., BAZÁN, C., et al. Graphene field-effect transistors as bioanalytical sensors: Design, operation and performance. *Analyst.* **2021**, vol.146(2), p.403 – 428 [cit. 2022-5-18]. ISSN 1364-5528. Available from: doi.org/10.1016/j.trac.2010.05.011.

[11] CHEN, T., LI, M., LIU, J., et al. π-π stacking interaction: a nondestructive and facile means in material engineering for bioapplications. *Crystal Growth & Design.* **2018**, vol.18(5), p.2765 – 2783 [cit. 2022-5-18]. ISSN 1528-7505. Available from: doi.org/10.1021/acs.cgd.7b01503.

[12] KWONG HONG TSANG, D., LIEBERTHAL, T.J., WATTS, C., et al. Chemically functionalised graphene FET biosensor for the label-free sensing of exosomes. *Scientific reports.* **2019**, vol.9(1), p.1 – 10 [cit. 2022-5-18]. ISSN 2045-2322.

[13] KHATAMI, S.H., VAKILI, O., AHMADI,N.,et al. Khatami, Seyyed Hossein, et al. Glucose oxidase: Applications, sources, and recombinant production. *Biotechnology and Applied Biochemistry.* **2021**,[cit. 2022-5-18]. Available from: doi.org/10.1002/bab.2165

[14] FERRI, S., KOJIMA, K., SODE, K.,et al. Review of glucose oxidases and glucose dehydrogenases: a bird's eye view of glucose sensing enzymes. *Journal of diabetes science and technology.* **2011**, vol.5(5), p.1068 – 1076 [cit. 2022-5-18]. ISSN 19322968. Available from: doi.org/10.1177/193229681100500507.

[15] JOHNSON, D., HILAL, N., BOWEN, W.R.,et al. Basic principles of atomic force microscopy. *Atomic force microscopy in process engineering.* **2009**, vol.5(5), p.1 – 30 [cit. 2022-5-18]. ISBN 9781856175173 . Available from: doi.org/10.1016/B978-1-85617-517-3.00001-8.

[16] MALARD, L., PIMENTA, M.A., DRESSELHAUS, G., et al. Raman spectroscopy in graphene. *Physics reports.* **2009**, vol.473(5), p.51 – 87 [cit. 2022-5-18]. ISSN 0370-1573. Available from: doi.org/10.1016/j.physrep.2009.02.003.

[17] REDDY, D., REGISTER, L., CARPENTER,G., et al. Graphene field-effect transistors. *Journal of Physics D: Applied Physics.* **2011**, vol.44(31), p.313001 [cit. 2022-5-18]. Available from: doi:10.1088/0022-3727/44/31/313001.

[18] ZHAN, B., LI, CH., YANG, J., et al. Graphene field-effect transistor and its application for electronic sensing. *Small.* **2014**, vol.10(20), p.4042 – 4065 [cit. 2022-5-18]. ISSN 1613-6829. Available from: doi.org/10.1002/smll.201400463.

[19] WU, G., TANG, X., MEYYAPPAN, M., et al. Chemical functionalization of graphene with aromatic molecule. *2015 IEEE 15th International Conference on Nanotechnology (IEEE-NANO).* **2014**, vol.10(20), p.1324 – 1327 [cit. 2022-5-18]. ISSN 1613-6829. Available from: doi.org/10.1109/NANO.2015.7388878.

[20] BANHART, F., KOTAKOSKI, J., KRASHENINNIKOV, A.V., et al. Structural defects in graphene. *ACS nano.* **2011**, vol.5(1), p.26 – 41 [cit. 2022-5-18]. ISSN 1936-086X. Available from: doi.org/10.1021/nn102598m.

[21] NOVOSELOV, K. S., GEIM A. K., MOROZOV, S. V., et al. Electric Field Effect in Atomically Thin Carbon Films. *Science*, vol. 306, p. 666 **2004**,[cit. 2021-5-17]. Available from: doi:10.1126/science.1102896.

[22] HUANG, Y., DONG, X., SHI, Y. , et al. Nanoelectronic biosensors based on CVD grown graphene *Nanoscale*, vol. 2, p. 1485–1488 **2010**,[cit. 2022-4-19]. Available from: doi:10.1039/C0NR00142B.

[23] WEI, S., HAO, Y., XU., C., et al. Transfer-free CVD graphene for highly sensitive glucose sensors. *Journal of Materials Science Technology* **2022**, vol. 37, p.71–76, [cit. 2022-4-19]. ISSN 2468-5194. Available from: doi.org/10.1016/j.jmst.2019.07.039.

[24] HUANG, C., HAO, Z., WANG., Z., et al.A fully integrated graphene-polymer field-effect transistor biosensing device for on-site detection of glucose in human urine. *Materials Today Chemistry* NATURE PUBLIDHING GROUP, **2022**, vol. 23, p.100635, [cit. 2022-4-19]. ISSN 2468-5194. Available from: doi.org/10.1016/j.mtchem.2021.100635.

[25] PING, J., VISHNUBHOTLA, R., VRUDHULA., A., et al.Scalable production of high-sensitivity, label-free DNA biosensors based on back-gated graphene field effect transistors. *ACS nano.* ACS PUBLICATIONS, **2016**, vol. 10(9), p.8700 – 8704 [cit. 2022-5-18]. ISSN 1936-086X. Available from: doi.org/10.1021/acsnano.6b04110.

[26] SAAL, K., SAMMELSELG, V., KUUSK, E., et al. Characterization of glucose oxidase immobilization onto mica carrier by atomic force microscopy and kinetic studies. *Biomolecular engineering.* **2002**, vol. 19(2), p.195 – 199 [cit. 2022-5-18]. ISSN 1389-0344. Available from: doi.org/10.1016/S1389-0344(02)00044-8.

[27] LIBERTINO, S., DIANNAZZO, F., AIELLO,V., et al. XPS and AFM characterization of the enzyme glucose oxidase immobilized on SiO2 surfaces. *Langmuir.* ACS PUBLICATIONS, **2008**, vol. 24(5), p.1965 – 1972 [cit. 2022-5-18]. ISSN 1389-0344. Available from: doi.org/10.1021/la7029664.

[28] WU, G., TANG, X., MEYYAPPAN, M., et al. Doping effects of surface functionalization on graphene with aromatic molecule and organic solvents. *Applied Surface Science.* **2017**, vol. 425, p.713 – 721 [cit. 2022-5-18]. ISSN 0169-4332. Available from: doi.org/10.1016/j.apsusc.2017.07.048.

[29] MAIDIN, N.N., RAHIM, R.A., HALIM, N.H.A., et al. Interaction of graphene electrolyte gate field-effect transistor for detection of cortisol biomarker. *Applied Surface Science.* **2018**, vol. 2045(1), p.020022 [cit. 2022-5-18]. ISSN 0169-4332. Available from: doi.org/10.1063/1.5080835.

[30] PONOR, CC BY-SA 4.0, [cit. 2022-5-18]. Available from: <https://creativecommons.org/licenses/by-sa/4.0>, via Wikimedia Commons

[31] SUPALOVA, Linda. Detection of Biochemical Substance using Graphene Sensir. *Bachelor's thesis.* Brno, **2021**. Brno University of Technology, Faculty of Mechanical Engineering, Institute of Physical Engineering.

Abbreviations

AFM	Atomic Force Microscopy
DI	Deionized Water
CVD	Chemical Vapor Deposition
CNT	Carbon nanotube
DMF	Dimethylformamide
FADH	Flavin adenine dinucleotide)
FET	Field-effect transistor
GFET	Graphene field-effect transistor
GluD	Glutamic dehydrogenase
GOx	Glucose oxidase
IPA	Isopropyl Alcohol
LOD	Limit of Detection
PMMA	Poly(methyl methacrylate)
PSE	1-pyrene butanoic acid succinimidyl
RIE	Reactive Ion Etching
SPM	Scanning Probe Microscopy
SWNT	Single-wall carbon nanotube